JACS
JOURNAL OF THE AMERICAN CHEMICAL SOCIETY

COMMUNICATION

pubs.acs.org/JACS

Probing the Reactivity and Electronic Structure of a Uranium(V) Terminal Oxo Complex

Skye Fortier,[†] Nikolas Kaltsoyannis,*[,‡] Guang Wu,[†] and Trevor W. Hayton*[,†]

[†]Department of Chemistry and Biochemistry, University of California, Santa Barbara, California 93106, United States

[‡]Christopher Ingold Laboratories, Department of Chemistry, University College London, 20 Gordon Street, London WC1H 0AJ, United Kingdom

Supporting Information

ABSTRACT: Treatment of the U(III)−ylide adduct U(CH$_2$PPh$_3$)(NR$_2$)$_3$ (**1**, R = SiMe$_3$) with TEMPO generates the U(V) oxo metallacycle [Ph$_3$PCH$_3$][U(O)(CH$_2$SiMe$_2$NSiMe$_3$)(NR$_2$)$_2$] (**2**) via O-atom transfer, in good yield. Oxidation of **2** with 0.85 equiv of AgOTf affords the neutral U(VI) species U(O)(CH$_2$SiMe$_2$NSiMe$_3$)(NR$_2$)$_2$ (**3**). The electronic structures of **2** and **3** are investigated by DFT analysis. Additionally, the nucleophilicity of the oxo ligands in **2** and **3** toward Me$_3$SiI is explored.

Metal oxo reactivity is often classified as either nucleophilic or electrophilic.[1] For the transition metals, these reactivity trends follow a relatively predictable pattern. In general, group 4 oxo ligands exhibit nucleophilic character, groups 5 and 6 can exhibit either nucleophilic or electrophilic reactivity, and later groups usually exhibit electrophilic character.[1−3] When it comes to the actinides, however, it is not clear which reactivity pattern will be operative as so few non-uranyl oxo complexes have been synthesized.[4−8] The highly electropositive nature of uranium suggests similarities with group 4 oxo chemistry, and preliminary reactivity studies imply that this is, in fact, the case.[4] For instance, Cp′$_2$U=O (Cp′ = 1,2,4-^{t}Bu$_3$C$_5$H$_2$) reacts with Me$_3$SiCl to give Cp′$_2$U(OSiMe$_3$)Cl, reactivity which is clearly nucleophilic.[9,10] Nonetheless, the rich redox chemistry of uranium suggests that its oxo reactivity may be more complicated than initial studies would indicate, and if actinide oxos are to be developed into useful catalysts, an improved understanding of this reactivity is critical.[11] In this communication, we report the synthesis, characterization, and reactivity of a rare terminal U(V) oxo complex in an attempt to address these issues.

We recently reported the synthesis of the U(IV) carbene complex U(=CHPPh$_3$)(NR$_2$)$_3$ (R = SiMe$_3$) which is generated by the one-electron oxidation of the U(III)−ylide adduct U(CH$_2$PPh$_3$)(NR$_2$)$_3$ (**1**), a transformation that is seemingly catalyzed by 10 mol % TEMPO (TEMPO = 2,2,6,6-tetramethylpiperidine-1-oxyl).[12] Interestingly, we have found that upon addition of a full equiv of TEMPO to **1** a new product is generated, namely the U(V) terminal oxo metallacycle [Ph$_3$PCH$_3$][U(O)(CH$_2$SiMe$_2$NSiMe$_3$)(NR$_2$)$_2$] (**2**), which can be isolated in 88% yield (Scheme 1). Surprisingly, under these conditions we see no evidence for the formation of the uranium carbene.

In the solid state, **2** crystallizes as a discrete cation−anion pair (Figure 1). The anionic U(V) center is ligated by a terminal oxo ligand, two silylamide ligands, and a silylamide-derived metallacycle,

Scheme 1

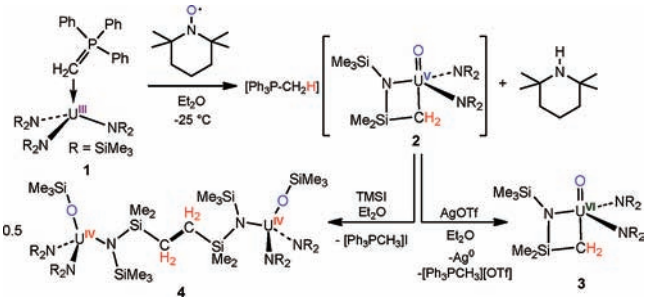

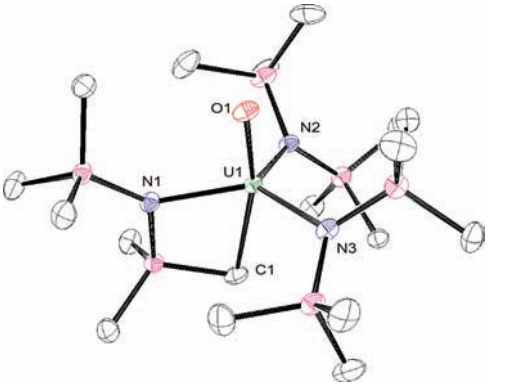

Figure 1. Solid-state molecular structure of [Ph$_3$PCH$_3$][U(O)(CH$_2$SiMe$_2$NSiMe$_3$)(NR$_2$)$_2$] (**2**) with 50% probability ellipsoids. Hydrogen atoms and [Ph$_3$PMe]$^+$ omitted for clarity.

presumably formed by deprotonation of a methyl group by the Wittig reagent. Interestingly, treatment of the related ylide adduct, U(CH$_2$PPh$_3$)(NN′$_3$) (NN′$_3$ = N(CH$_2$CH$_2$NSiMe$_2$^{t}Bu)$_3$) with Me$_3$NO also generates a U(V) oxo complex U(O)(NN′$_3$); however, this complex has not been structurally characterized.[8]

The U(V) center in **2** possesses a U−O$_{oxo}$ bond length of U1−O1 = 1.847(2) Å and a U−C$_{alkyl}$ distance of U1−C1 = 2.427(3) Å (Table 1). The oxo ligand coordinates *trans* to the U−C$_{alkyl}$ bond, providing a O−U−C bond angle of O1−U1−C1 = 165.8(1)°. The U−O$_{oxo}$ distance of **2** is comparable to those found for [U(O)(tacn(OAr^R)$_3$)] (av. U−O = 1.85 Å; R = ^{t}Bu, Ad)[7]

Received: June 30, 2011
Published: August 18, 2011

Table 1. Selected Bond Lengths (Å) and Angles (°) for 2 and 3 Obtained Experimentally and Computationally

	2		3	
	exp	calcd	exp	calcd
U−O	1.847(2)	1.846	1.800(2)	1.831
U−C	2.427(3)	2.462	2.319(2)	2.360
O−U−C	165.8(1)	163.8	167.02(8)	164.4

and $Cp^*_2U(O)(O\text{-}2,6\text{-}{}^iPr_2C_6H_3)$ (U−O = 1.859(6) Å),[6] the only other U(V) mono-oxo complexes that have been structurally characterized. Additionally, the U−C_{alkyl} distance in **2** is identical to that found for the related U(V) nitrido complex $(NR_2)_2U(\mu\text{-}N)(\mu\text{-}CH_2SiMe_2NSiMe_3)U(NR_2)_2$ (U−C = 2.427(8) Å).[13]

The ^{1}H NMR spectrum of **2** in C_6D_6 exhibits four resonances assignable to the anion at −6.07, −4.15, 14.19, and 36.91 ppm, in a 36:9:6:2 ratio, respectively, consistent with its solid-state molecular structure. The resonances for the $[Ph_3PCH_3]^+$ cation appear in the ^{1}H NMR spectrum at 8.38, 8.87, 9.20, and 16.14 ppm in a 3:6:6:3 ratio, respectively, while a single peak is observed in the $^{31}P\{^1H\}$ NMR spectrum at 29.9 ppm. Complex **2** exhibits an effective magnetic moment of 1.97 μ_B at 300 K, and 1.47 μ_B at 4 K, as determined by SQUID magnetometry. These values are comparable to the effective magnetic moments found for $[U^V(O)(tacn(OAr^R)_3)]$ (e.g., μ_{eff} = 1.98 μ_B, R = ^{t}Bu; μ_{eff} = 1.92 μ_B, R = Ad at 300 K).[7] The X-band EPR spectrum of complex **2** at 8 K also supports the 5+ oxidation state assignment (see the Supporting Information (SI)).

Monitoring the in situ formation of **2** by ^{1}H NMR spectroscopy reveals the formation of tetramethylpiperidine (TMPH), suggesting that the TMP· radical is transiently formed upon O-atom transfer and subsequently abstracts H· from the solvent to give TMPH. To test this, the addition of TEMPO to **1** was conducted in the presence of 9,10-dihydroanthracene. Under these conditions, the formation of 9,9′,10,10′-tetrahydro-9,9′-bianthracene, a product of H$^\bullet$ abstraction from 9,10-dihydroanthracene,[14] is observed in the reaction mixture (see the SI), consistent with the proposed reaction pathway. Oxygen atom transfer from TEMPO is somewhat rare, given that nitroxyl radicals usually act as one-electron oxidants.[15] Moreover, the synthesis of **2** calls into question the role of TEMPO in the original formation of the U(IV) carbene $U(=CHPPh_3)(NR_2)_3$,[12] and suggests instead that complex **2** (and not TEMPO) catalyzes the conversion of **1** to $U(=CHPPh_3)(NR_2)_3$. Consistent with this hypothesis, addition of 10 mol % of **2** to a solution of **1** dramatically increases the rate of conversion to $U(=CHPPh_3)(NR_2)_3$, versus the uncatalyzed reaction (Figure S11). In light of this, it is likely that the addition of a substoichiometric amount of TEMPO to **1** generates **2**, which is the actual catalyst. Indeed, hydrogen atom abstraction by metal oxo complexes is well-established and central to many M=O mediated oxidations.[16]

The redox properties of **2** were assessed using cyclic voltammetry. In THF at room temperature, **2** displays a reversible oxidation feature at −0.85 V (vs $[Cp_2Fe]^{0/+}$) assignable to a U(VI)/U(V) redox couple. This potential is nearly 400 mV lower than that of the related U(V) imido $U(NR)(NR_2)_3$ ($E_{1/2}$ = −0.41 V vs $[Cp_2Fe]^{0/+}$),[17] likely owing to the anionic charge in **2**. Scanning to lower potentials produces an irreversible reduction feature at −2.6 V which presumably arises from the formation of an unstable U(IV) complex.

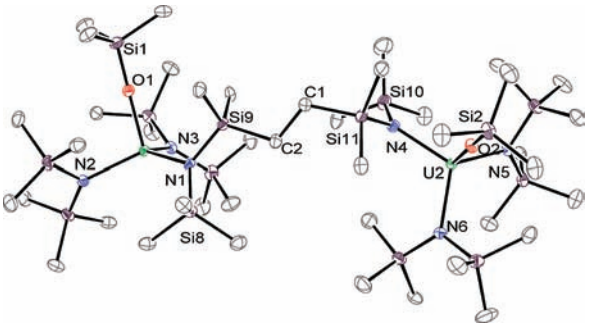

Figure 2. Solid-state molecular structure of $[U(OSiMe_3)(NR_2)_2]_2(RNSiMe_2CH_2)_2$ (**4**) with 50% probability ellipsoids.

Consistent with the electrochemical data, treatment of **2** with 0.85 equiv of AgOTf affords the U(VI) derivative $U(O)(CH_2SiMe_2NSiMe_3)(NR_2)_2$ (**3**) in 46% yield (Scheme 1). Alternatively, **3** can be synthesized by direct addition of TEMPO to the previously reported metallacycle $U(CH_2SiMe_2NSiMe_3)(NR_2)_2$;[18] however, this route only provides **3** in low yield. The ^{1}H NMR spectrum of **3** in C_6D_6 displays four resonances at −1.89, 0.60, 0.65, and 0.83 ppm in a 2:9:36:6 ratio, respectively, in line with its formulation. Additionally, the $^{13}C\{^1H\}$ NMR spectrum of **3** exhibits three resonances at 6.00, 7.02, and 7.25 ppm, corresponding to the methyl environments, while the methylene carbon is highly deshielded, appearing at 317.4 ppm.

Crystallographic analysis of **3** reveals that the $[O{=}U{-}CH_2]^{3+}$ fragment retains a *trans* arrangement (O1−U1−C1 = 167.02(8)°) in the solid state (see SI). The U−O_{oxo} bond length in **3** decreases to 1.800(2) Å, consistent with the contraction anticipated to occur upon oxidation from U(V) to U(VI).[19] For comparison, this bond is slightly shorter than the U−O_{oxo} distance of $Cp^*_2U(O)(N\text{-}2,6\text{-}{}^iPr_2C_6H_3)$[6] (U−O = 1.844(4) Å) but similar to that of $[Ph_4P][U(O)Cl_5]$ (U−O = 1.76(1) Å).[20] Complex **3** also features a U1−C1 bond distance of 2.319(2) Å. Notably, **3** is the only example of a non-uranyl complex to feature a structurally characterized U(VI)−C_{alkyl} bond.[21,22] The U−C distance of **3** is similar to the calculated U−C distances of $U(CH_2SiMe_3)_6$ (2.353−2.377 Å).[23] Additionally, the U−C bond length in **3** is substantially shorter than the U−C bond in the uranyl alkyl $UO_2(SCHS)(OTf)(OEt_2)$ (U−C = 2.647(12) Å), and even the uranyl carbene $UO_2(SCS)(py)_2$ (U−C = 2.430(6) Å) ($[SCS]^{2-}$ = $[C(Ph_2PS)_2]^{2-}$),[21] but it is similar to the U=C distances found in $Cp_3U{=}CHPMe_2Ph$ (2.29(3) Å)[24] and $Cp_2U(C(PPh_2S)_2$ (2.336(4) Å).[25]

We have also investigated the reactivity of the oxo ligands in **2** and **3**. For example, addition of the nucleophile PPh_3 to either **2** or **3** does not result in any reaction. Similarly, **2** does not react with the C−H bonds of 9,10-dihydroanthracene. In contrast, treatment of **2** with the electrophile Me_3SiI in Et_2O results in a rapid color change and precipitation of $[Ph_3PCH_3][I]$ as a white solid. From this reaction mixture, the U(IV) silyloxide dimer $[U(OSiMe_3)(NR_2)_2]_2(RNSiMe_2CH_2)_2$ (**4**) can be isolated in 82% yield (Scheme 1). Interestingly, upon addition of 1 equiv of Me_3SiI to **3**, no immediate reaction is observed. Upon standing for 48 h, however, a mixture of intractable products is eventually generated.

Crystallographic analysis of **4** (Figure 2) reveals a tetrahedral geometry about each uranium center, a consequence of homolytic cleavage of the metallacycle U−C bond. The $OSiMe_3$ ligand in **4**, formed by silylation of the terminal oxo, exhibits a much longer U−O bond length (U1−O1 = 2.102(2) Å) than that

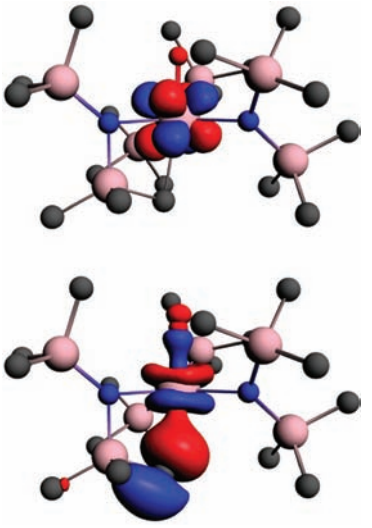

Figure 3. Representations of the singly occupied HOMO (upper) and α spin HOMO−1 (lower) of **2** (H atoms omitted for clarity). The isosurface plot level is 0.05.

observed in **2** or **3**, revealing a significant reduction in bond order. Additionally, the length of the new C−C bond (C1−C2 = 1.554(4) Å), formed by coupling of metallacyle ligands, is typical for sp^3-hybridized carbon atoms. To account for the formation of **4**, we believe that coordination of the Me_3Si^+ cation to the oxo group in **2** reduces its π-donating capacity, thereby increasing the U(V)/U(IV) redox potential and making the U(V) center a substantially better oxidant. As a result, the U(V) center oxidizes the U−C bond, generating the methylene radical. Coupling of two methylene radicals results in formation of the $-CH_2-CH_2-$ bridge that links the two U(IV) centers of **4**. This transformation echoes the reductive silylation of $UO_2(^{Ar}acnac)_2$ ($^{Ar}acnac$ = Ar*N*C(Ph)CHC(Ph)*O*; Ar = 3,5-^{t}Bu$_2$C$_6$H$_3$) by Me_3SiI, which also exhibits oxo silylation marked by ligand oxidation and $1e^-$ reduction of the uranium center.[26,27]

The silylation of the oxo group in **4** reveals the nucleophilic character of the oxo ligand, consistent with early metal behavior. However, the subsequent $1e^-$ reduction of the uranium center, brought about by U−C bond homolysis, is at odds with the silylation chemistry established for early transition metal oxo complexes.[28−32] Instead, the reduction of **2** is akin to the $1e^-$ and $2e^-$ redox changes expected for a mid- to late-metal oxo.[3,33] Thus, the conversion of **2** into **4** does not fit within the traditional electrophilic vs nucleophilic reactivity manifold observed for the transition metals, challenging our ability to easily classify the reactivity of this oxo ligand.

To better understand the electronic structure of complexes **2** and **3**, DFT calculations were performed at the scalar relativistic GGA level. The computed U−O and U−C bond lengths, and the O−U−C angles, collected in Table 1, reveal good agreement between experiment and theory. The U−O distance in **2** is reproduced well by the calculation, though the reduction in this metric from U(V) to U(VI) is underestimated theoretically. Calculation slightly overestimates the U−C distances, but accurately reproduces the ca. 0.1 Å shortening on oxidation.

Mulliken population analysis reveals that the singly occupied HOMO of **2** is >95% U 5f in character (Figure 3), while **3** has, as expected, no metal-localized valence electrons. The partial atomic charges for the uranium and oxygen atoms are given in Table 2.

Table 2. Selected Partial Atomic Charges q and U−O and U−C Bond Orders for Complexes 2, 3, $UO_2^{+/2+}$, and $[UO_2(OH_2)_2(OH)_2]^{0/-}$

compound	oxidation state	q_U	q_O	U−O	U−C
2	V	+1.99	−0.82	2.29	0.84
3	VI	+2.34	−0.78	2.33	0.97
UO_2^+	V			2.54	
UO_2^{2+}	VI			2.69	
$[UO_2(OH_2)_2(OH)_2]^-$	V			2.22	
$UO_2(OH_2)_2(OH)_2$	VI			2.31	

The uranium charge increases significantly from **2** to **3**, and the increased U/O charge difference is in agreement with the concomitant bond length reduction. Furthermore, the charge buildup on the oxygen atom in **2** vs **3**, while small, is consistent with the former's nucleophilicity.

Figure 3 shows that the HOMO−1 of **2** is of predominant U−C σ-bonding character, with some U−O σ. This is also broadly true of the HOMO of **3** (see the SI). However, population analysis indicates that there is significant (ca. 20%) N p involvement in the latter orbital, and also that U−O bonding character is spread over several highly delocalized MOs in both **2** and **3**. Hence, to gain clearer insight into the effect of oxidation on these bonds, we have calculated the Gopinathan−Jug U−O and U−C bond orders. These are collected in Table 2, together with comparative U−O data for bare uranyl(V/VI) and $[UO_2(OH_2)_2(OH)_2]^{0/-}$, computed here using the same methodology as for **2** and **3**. There is a slight increase in the U−O bond order from **2** to **3**, and a larger increase in that for the U−C bond. In **3**, the latter approaches unity, suggestive of a single bond, while the U−O bond order lies in between a double and triple. The U−O data for **2** and **3** are very similar to those for the analogously charged systems with all-oxygen coordination and, interestingly, rather lower than for the bare uranyl, suggesting that coordination in the equatorial plane significantly weakens the axial U−O bond.

In summary, the U(III)−ylide adduct $U(CH_2PPh_3)(NR_2)_3$ (R = $SiMe_3$) is readily oxidized by TEMPO to give a U(V) terminal oxo complex, $[Ph_3PCH_3][U(O)(CH_2SiMe_2NSiMe_3)(NR_2)_2]$, via O-atom transfer from the nitroxyl radical. DFT analysis indicates that the unpaired electron in the anion is almost entirely U 5f in character, and that the U−O bond order is in between that of a double and a triple bond. One-electron oxidation of this U(V) complex produces the neutral U(VI) species, $U(O)(CH_2SiMe_2NSiMe_3)(NR_2)_2$, which calculation shows to have an electronic structure similar that of the anion but without the U 5f electron and with a slightly larger U−O bond order. Silylation of the oxo ligand in the U(V) complex results in U−C bond homolysis and C−C bond coupling to form $[U(OSiMe_3)(NR_2)_2]_2(RNSiMe_2CH_2)_2$. The latter reaction is consistent with nucleophilic metal oxo behavior, but the unanticipated reduction of the metal center suggests that the actinides will be a fruitful arena for uncovering new modes of reactivity for metal−ligand multiple bonds. We intend to further explore the reactivity of $U(CH_2PPh_3)(NR_2)_3$ as a means to synthesize other uranium complexes featuring metal−ligand multiple bonds.

■ ASSOCIATED CONTENT

Supporting Information. Experimental procedures, crystallographic details (as CIF files), spectral data for **1**−**4**, and

computational details for **2** and **3**. This material is available free of charge via the Internet at http://pubs.acs.org.

AUTHOR INFORMATION

Corresponding Author
hayton@chem.ucsb.edu; n.kaltsoyannis@ucl.ac.uk

ACKNOWLEDGMENT

We thank the University of California, Santa Barbara, and the Department of Energy (BES Heavy Element Program) for financial support of this work. We are grateful to UCL for computing resources via the Research Computing "Legion" cluster and associated services, and the UK EPSRC for computing resources under grant GR/S06233 and via its National Service for Computational Chemistry Software (http://www.nsccs.ac.uk). We also thank Wayne W. Lukens, Jr., at LBNL for recording the EPR spectrum of **2**.

REFERENCES

(1) Nugent, W. A.; Mayer, J. M. *Metal-Ligand Multiple Bonds*; John Wiley & Sons: New York, 1988.
(2) Holm, R. H. *Chem. Rev.* **1987**, *87*, 1401–1449.
(3) Gunay, A.; Theopold, K. H. *Chem. Rev.* **2010**, *110*, 1060–1081.
(4) Hayton, T. W. *Dalton Trans.* **2010**, *39*, 1145–1158.
(5) Kraft, S. J.; Walensky, J.; Fanwick, P. E.; Hall, M. B.; Bart, S. C. *Inorg. Chem.* **2010**, *49*, 7620–7622.
(6) Arney, D. S. J.; Burns, C. J. *J. Am. Chem. Soc.* **1993**, *115*, 9840–9841.
(7) Bart, S. C.; Anthon, C.; Heinemann, F. W.; Bill, E.; Edelstein, N. M.; Meyer, K. *J. Am. Chem. Soc.* **2008**, *130*, 12536–12546.
(8) Roussel, P.; Boaretto, R.; Kingsley, A. J.; Alcock, N. W.; Scott, P. *J. Chem. Soc., Dalton Trans.* **2002**, 1423–1428.
(9) Barros, N.; Maynau, D.; Maron, L.; Eisenstein, O.; Zi, G. F.; Andersen, R. A. *Organometallics* **2007**, *26*, 5059–5065.
(10) Zi, G.; Jia, L.; Werkema, E. L.; Walter, M. D.; Gottfriedsen, J. P.; Andersen, R. A. *Organometallics* **2005**, *24*, 4251–4264.
(11) Fox, A. R.; Bart, S. C.; Meyer, K.; Cummins, C. C. *Nature* **2008**, *455*, 341–349.
(12) Fortier, S.; Walensky, J. R.; Wu, G.; Hayton, T. W. *J. Am. Chem. Soc.* **2011**, *133*, 6894–6897.
(13) Fortier, S.; Wu, G.; Hayton, T. W. *J. Am. Chem. Soc.* **2010**, *132*, 6888–6889.
(14) Arnold, P. L.; Pecharman, A.-F.; Hollis, E.; Yahia, A.; Maron, L.; Parsons, S.; Love, J. B. *Nat. Chem.* **2010**, *2*, 1056–1061.
(15) Lippert, C. A.; Soper, J. D. *Inorg. Chem.* **2010**, *49*, 3682–3684.
(16) Waidmann, C. R.; Zhou, X.; Tsai, E. A.; Kaminsky, W.; Hrovat, D. A.; Borden, W. T.; Mayer, J. M. *J. Am. Chem. Soc.* **2009**, *131*, 4729–4743.
(17) Burns, C. J.; Smith, W. H.; Huffman, J. C.; Sattelberger, A. P. *J. Am. Chem. Soc.* **1990**, *112*, 3237–3239.
(18) Simpson, S. J.; Turner, H. W.; Andersen, R. A. *Inorg. Chem.* **1981**, *20*, 2991–2995.
(19) Shannon, R. D. *Acta Crystallogr.* **1976**, *A32*, 751–767.
(20) O'Grady, E.; Kaltsoyannis, N. *J. Chem. Soc., Dalton Trans.* **2002**, 1233–1239.
(21) Tourneux, J.-C.; Berthet, J.-C.; Cantat, T.; Thuery, P.; Mezailles, N.; Ephritikhine, M. *J. Am. Chem. Soc.* **2011**, *133*, 6162–6165.
(22) Sarsfield, M. J.; Steele, H.; Helliwell, M.; Teat, S. J. *Dalton Trans.* **2003**, 3443–3449.
(23) Fortier, S.; Walensky, J.; Wu, G.; Hayton, T. W. *J. Am. Chem. Soc.* **2011**, *133*, 11732–11743.
(24) Cramer, R. E.; Maynard, R. B.; Paw, J. C.; Gilje, J. W. *J. Am. Chem. Soc.* **1981**, *103*, 3589–3590.
(25) Tourneux, J.-C.; Berthet, J.-C.; Thuery, P.; Mezailles, N.; Le Floch, P.; Ephritikhine, M. *Dalton Trans.* **2010**, *39*, 2494–2496.
(26) Brown, J. L.; Wu, G.; Hayton, T. W. *J. Am. Chem. Soc.* **2010**, *132*, 7248–7249.
(27) Brown, J. L.; Mokhtarzadeh, C. C.; Lever, J. M.; Wu, G.; Hayton, T. W. *Inorg. Chem.* **2011**, *50*, 5105–5112.
(28) Parkin, G.; Bercaw, J. E. *J. Am. Chem. Soc.* **1989**, *111*, 391–393.
(29) Odom, A. L.; Mindiola, D. J.; Cummins, C. C. *Inorg. Chem.* **1999**, *38*, 3290–3295.
(30) Jayarathne, U.; Chandrasekaran, P.; Jacobsen, H.; Mague, J. T.; Donahue, J. P. *Dalton Trans.* **2010**, *39*, 9662–9671.
(31) Howard, W. A.; Waters, M.; Parkin, G. *J. Am. Chem. Soc.* **1993**, *115*, 4917–4918.
(32) Howard, W. A.; Trnka, T. M.; Waters, M.; Parkin, G. *J. Organomet. Chem.* **1997**, *528*, 95–121.
(33) England, J.; Guo, Y.; Farquhar, E. R.; Young, V. G., Jr.; Munck, E.; Que, L., Jr. *J. Am. Chem. Soc.* **2010**, *132*, 8635–8644.